JOC The Journal of Organic Chemistry

Article

pubs.acs.org/joc

Ion-Pairing Crystal Polymorphs of Interlocked [2 + 1]-Type Receptor–Anion Complexes

Ryohei Yamakado,[†] Ryuma Sato,[‡] Yasuteru Shigeta,*[,‡] and Hiromitsu Maeda*[,†]

[†]Department of Applied Chemistry, College of Life Sciences, Ritsumeikan University, Kusatsu 525-8577, Japan

[‡]Department of Physics, Graduate School of Pure and Applied Sciences, University of Tsukuba, Tsukuba 305-8577, Japan

Supporting Information

ABSTRACT: The formation of a solid-state totally charge-segregated assembly (polymorph **A**) of negatively charged layers comprising [2 + 1]-type Cl^- complexes of an arylethynyl-substituted dipyrrolyldiketone boron complex and positively charged layers of tetrabutylammonium (TBA) cations has already been reported. The formation of two new crystalline polymorphs (polymorphs **B** and **C**), in addition to polymorph **A**, is reported in this study. Both polymorphs **B** and **C** formed charge-by-charge assemblies, and the dihedral angles between two receptor units in the interlocked complexes depended on the geometries of TBA cations and the resulting packing structures. Two nonorthogonally arranged planes induced *P*- and *M*-form chiral geometries, providing diverse arrangements of chiral species according to crystal polymorphs. Furthermore, the stabilities of the three polymorphs were examined by interfragment interaction energies, which were calculated by *ab initio* electronic structure calculations using the fragment molecular orbital (FMO) method.

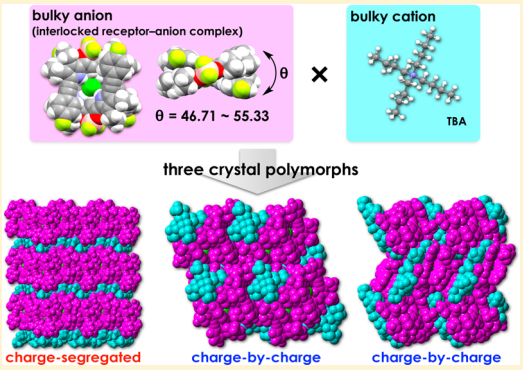

INTRODUCTION

Charged π-electronic systems form ion pairs when they combine with corresponding counterions, providing ordered assemblies, mainly through interionic interactions, that result in nanoscale architectures.[1] As shown in Figure 1a, ion-pairing assembly modes can be categorized as charge-by-charge and charge-segregated assemblies according to the arrangement of charged species. A charge-by-charge assembly is defined as the mode comprising alternately stacking positively and negatively charged species, whereas a charge-segregated assembly results from the stacking of identically charged species by overcoming electrostatic repulsions. Designs of π-electronic ions with appropriate sizes, geometries, and electron densities are required to achieve ordered arrangements. These ordered assemblies are formed via a variety of interactions using π-electronic systems along with peripheral substituents. However, π-electronic anions are not easily synthesized due to their electron-rich characteristics that facilitate their transformation into other species.[2] Therefore, anion binding by electronically neutral π-electronic molecules is an effective strategy for the preparation of negatively charged π-electronic systems.

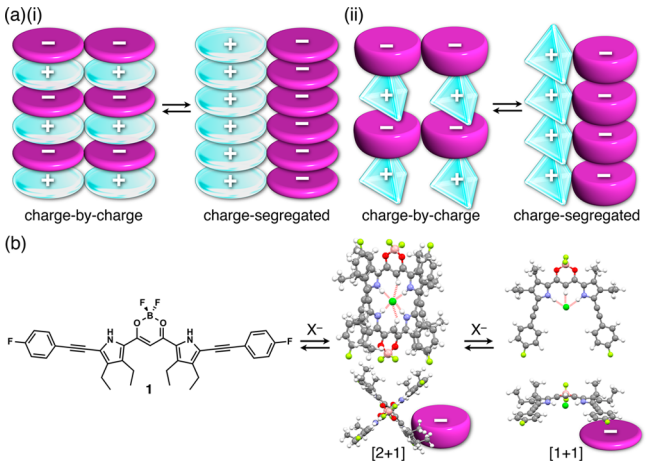

Figure 1. (a) Conceptual diagrams of ion-pairing assemblies based on (i) planar and (ii) bulky ions; (b) ethynyl-substituted anion-responsive π-electronic molecule **1**, providing interlocked [2 + 1]- and planar [1 + 1]-type complexes with anions (Cl^- and Br^-) represented as AM1 models (top and side views).

Dipyrrolyldiketone boron complexes are electronically neutral anion-responsive π-systems (anion receptors) that can form anion complexes. These anion complexes can yield diverse dimension-controlled assemblies such as supramolecular gels and thermotropic liquid crystals when they combine with appropriate cations.[3] The α-arylethynyl-substituted **1** possesses a fluorine moiety at the terminal *para* aryl position and exhibits fascinating anion-binding behavior: the formation of an interlocked [2 + 1]-type complex consisting of two receptors and one anion in addition to the planar [1 + 1]-type complex, which is also seen in other derivatives (Figure 1b).[4] Interlocked

Received: July 14, 2016
Published: August 15, 2016

DOI: 10.1021/acs.joc.6b01688
J. Org. Chem. 2016, 81, 8530–8536

[2 + 1]-type complexes were formed in equilibrium solutions from **1** in the presence of a small amount of a guest anion, such as Cl^- under the following conditions: relatively high concentrations, low temperature, and less polar solvents. At 1 mM at −50 °C in CD_2Cl_2, [2 + 1]-type $\mathbf{1}_2{\cdot}Cl^-$ was found to occur as a major species upon the addition of 0.35−4.85 equiv of Cl^-.[5] Further addition of Cl^- resulted in the formation of a larger amount of the [1 + 1]-type $\mathbf{1}{\cdot}Cl^-$. $\mathbf{1}_2{\cdot}Cl^-$ enables multiple hydrogen bonding to a guest anion via interaction sites on **1**, even though two receptor units should be assembled as a single complex. Few examples of interlocked [2 + 1]-type anion complexes have been reported.[6] Therefore, it was remarkable to find that arylethynyl moieties in dipyrrolyldiketone BF_2 complexes can provide interlocked [2 + 1]-type complexes using larger anion-binding cavities.

Dihedral angles between two receptor molecules in the interlocked [2 + 1]-type anion complexes can be optimized by varying the conditions. These dihedral angles are determined by geometry variation of the accompanying complex-bound cations, providing different sizes of [2 + 1]-type complexes and their resultant assembled structures. Thus far, eight types of crystal states as ion-pairing assemblies of $\mathbf{1}_2{\cdot}Cl^-$ and $\mathbf{1}_2{\cdot}Br^-$ have been prepared. Notably, several ion pairs of $\mathbf{1}_2{\cdot}Cl^-$ yielded totally charge-segregated assemblies in their crystal states, wherein the layers of identically charged species alternately stacked.[4] As an example, a totally charge-segregated assembly was constructed as an ion pair of $\mathbf{1}_2{\cdot}Cl^-$ and tetrabutylammonium (TBA) cation.[4a] By surrounding the guest anion in [2 + 1]-type complexes with two π-electronic molecules, their collective negative charge is delocalized. This reduces the electrostatic repulsion between identically charged species, which in this case are anions, resulting in the formation of anionic and cationic layers. Thus, various arrangements of charged species were obtained by modifying the receptors and by combining them with cations of various geometries and electronic states. Ion-pairing assemblies can be formed where oppositely and identically charged species are arranged appropriately in terms of distance and orientation. The characteristics of assembly modes, including charge-by-charge and charge-segregated assemblies, are determined by the interactions between their constitutive charged species, charge distributions, and resulting total stabilities. A better understanding of the characteristics of the assembly modes can be achieved based on the characteristics of ion-pairing systems comprising the same charged species (cations and anions), such as ion-pairing crystal polymorphs.[7] Many reports discuss the solid-state properties and stabilities of crystal polymorphs comprising electronically neutral molecules.[8] However, it is challenging to discuss the diverse arrangements of charged species in detail due to a limited amount of published research on the characteristics of ion-pairing crystal polymorphs, with the exception of those containing salt bridges and metal ions.[9] This report discusses the formation and characteristics of two new crystal polymorphs of $\mathbf{1}_2{\cdot}Cl^-{-}TBA^+$, assignable to charge-by-charge assemblies, and compares them with the previously obtained totally charge-segregated structure.[4a] This is the first report that discusses the preparation of both charge-by-charge and charge-segregated assemblies as polymorphs and compares their stabilities by theoretical calculations. This study contributes to the understanding of designed ion-pairing assemblies.

RESULTS AND DISCUSSION

Crystal Polymorphs of $\mathbf{1}_2{\cdot}Cl^-{-}TBA^+$. Polymorphs, some of which are metastable, are generally obtained by different processes of nucleation and crystal growth.[7] The X-ray structure of $\mathbf{1}_2{\cdot}Cl^-{-}TBA^+$ labeled as polymorph **A** was obtained from a single crystal by slow vapor diffusion of *n*-hexane into an EtOAc solution of $\mathbf{1}_2{\cdot}Cl^-{-}TBA^+$ as a mixture of **1** and TBACl in a 2:1 ratio.[4a] New polymorphs, labeled as **B** and **C**, were obtained by adding alcohols to an EtOAc solution of a 1:1 mixture of **1** and TBACl. Polymorph **C** was obtained as a red prism by adding (*rac*)-(±)-2-butanol (17% (v/v)) to an EtOAc solution of a 1:1 mixture of **1** and TBACl. Crystallization using (*S*)-(+)-2-butanol, instead of (*rac*)-(±)-2-butanol, resulted in the formation of polymorph **A**. Polymorph **B** was formed as a red prism through crystallization by slow vapor diffusion of *n*-hexane into an EtOAc and (*S*)-(−)-2-methyl-1-butanol (5/1 (v/v)) mixture, containing a 1:1 mixture of **1** and TBACl. These observations suggested that the obtained polymorph structures depended on the chirality and geometry of each alcohol used for crystallizations. Therefore, the impact of alcohol structure on crystallization mechanisms is under further investigation. The crystal colors of the three polymorphs were similar, whereas their crystal shapes differed. Crystals of polymorphs **A** and **B** were highly anisotropic rectangular shapes, and those of polymorph **C** were parallelogram-shaped plates (Figure 2a).

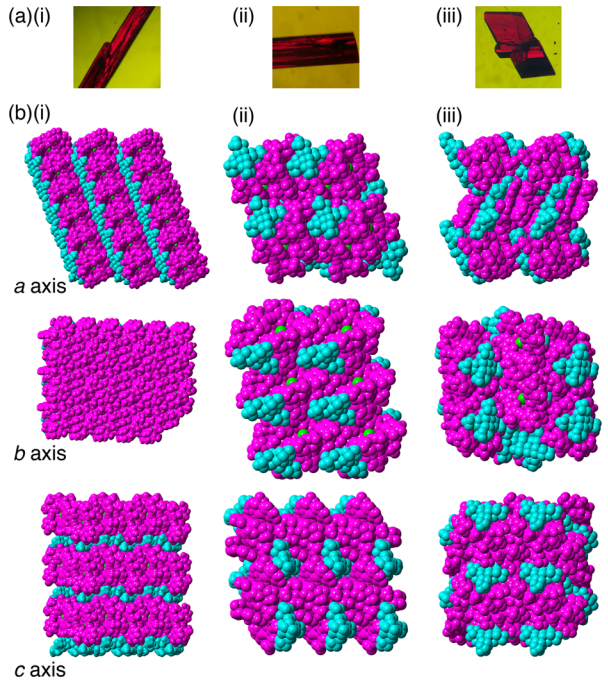

Figure 2. (a) Photographs of single crystals and (b) packing diagrams (the view along the *a* (top), *b* (middle), and *c* (bottom) axes) of polymorphs (i) **A**, (ii) **B**, and (iii) **C**, wherein the magenta- and cyan-colored parts represent the anion (receptor−Cl^- complexes) and cation species, respectively.

Crystal Structures of $\mathbf{1}_2{\cdot}Cl^-{-}TBA^+$. Crystallographic characteristics of the three polymorphs are summarized in Table 1. Polymorphs **A** and **B** were crystallized in the triclinic $P\bar{1}$ system, whereas polymorph **C** was crystallized in the monoclinic $P2_1/n$ system. Two independent receptor−anion complexes and cations were observed in polymorph **A** (Figure

DOI: 10.1021/acs.joc.6b01688
J. Org. Chem. 2016, 81, 8530−8536

Table 1. Crystallographic Details for Three Polymorphs of 1_2·Cl⁻−TBA⁺

	A[a]	B	C
formula	$C_{35}H_{31}BF_4N_2O_2Cl·C_{16}H_{36}N$		
fw	1474.76		
crystal size	0.08 × 0.05 × 0.01	0.12 × 0.06 × 0.06	0.24 × 0.20 × 0.10
crystal system	triclinic	triclinic	monoclinic
space group	$P\bar{1}$ (no. 2)	$P\bar{1}$ (no. 2)	$P2_1/n$ (no. 14)
a, Å	16.923(5)	13.613(2)	16.0367(18)
b, Å	21.296(8)	17.506(5)	18.5146(19)
c, Å	23.710(9)	17.927(5)	27.063(3)
α, deg	111.142(11)	108.335(12)	90
β, deg	92.281(13)	101.007(4)	92.969(4)
γ, deg	90.156(9)	90.798(4)	90
V, Å^3	7962(5)	3968.1(17)	8024.6(15)
ρ_{calcd}, g cm^{-3}	1.230	1.234	1.221
Z	4	2	4
T, K	93(2)	93(2)	93(2)
μ, mm^{-1}	1.014	1.017	1.006
no. of reflns	99 682	102 998	53 418
no. of unique	27 000	14 279	14 567
variables	2237	987	967
λ, Å (Cu Kα)	1.54187	1.54187	1.54187
R_1	0.0803	0.0305	0.0340
wR_2	0.1895	0.0831	0.1188
GOF	1.034	1.063	1.071

[a]Reference 4a.

2b). The hydrogen-bonding geometries in 1_2·Cl⁻ are summarized in Figure 3 and Table 2. Distances between pyrrole NH and Cl⁻, $d_{N(-H)\cdots Cl}$ = 3.26−3.39 Å, are shorter than those between bridged CH and Cl⁻, $d_{C(-H)\cdots Cl}$ = 3.45−3.55 Å. Although there are no significant differences between the N/C(−H)···Cl distances of the polymorphs, the dihedral angles between two interlocked receptor core planes, which consist of 15 sp^2 atoms per plane, are quite different: θ = 51.19/51.22°, 46.71°, and 55.33° for polymorphs **A**, **B**, and **C**, respectively (Figure 3). A previous study[4a] found that the dihedral angles, which are significantly correlated with the sizes of [2 + 1]-type complexes, can be controlled to fit their sizes to those of counter cations. However, in the three polymorphs, the sizes of the TBA cation in the solid state were almost equal with slight differences according to the packing structures. Therefore, various potential dihedral angles of 1_2·Cl⁻ enable the formation of polymorphs with different arrangements of charged species. Polymorph **A** contains a totally charge-segregated assembly, wherein positively and negatively charged species form respective layered structures. However, polymorphs **B** and **C** form charge-by-charge assemblies, wherein the TBA cation is located in the cavity of 1_2·Cl⁻. Although the TBA cation is located in close proximity to Cl⁻ in polymorph **B**, no specific interactions between these oppositely charged species were observed. However, interactions between Cl⁻ and the CH moieties neighboring TBA-N in polymorph **C** were apparent with $d_{TBA\text{-}C(-H)\cdots Cl}$ distances of 3.72 and 3.92 Å.

Contributions of $\pi-\pi$ stacking interactions in the packing structures play a crucial role in the formation of the assemblies (Figure 4). Even though the assembly modes of the polymorphs are significantly different, polymorphs **A** and **B** contain similar packing structures of 1_2·Cl⁻, wherein two kinds of $\pi-\pi$ stacking interactions can be observed along two axes. In polymorph **A** (Figure 4a), the phenylethynyl moieties stack in

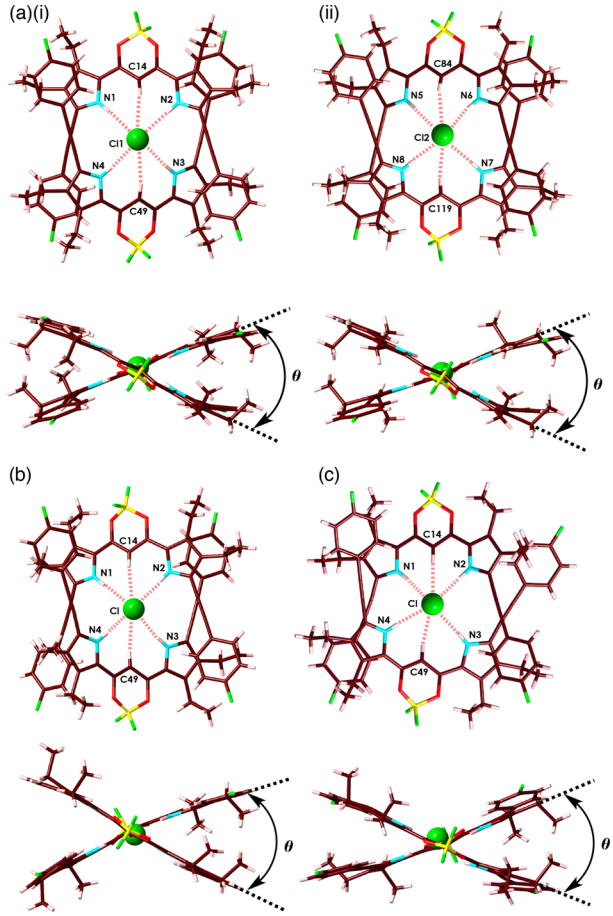

Figure 3. Crystal structures of [2 + 1]-type complexes in 1_2·Cl⁻−TBA⁺, representing hydrogen-bonding interactions, in polymorphs (a) **A** with two independent structures (i,ii),[4a] (b) **B**, and (c) **C**. Atom color code: brown, yellow, green, blue, and red refer to carbon, boron, fluorine, nitrogen, and oxygen, respectively.

an opposite (anti-) direction along the c axis, with a dihedral angle of 0° between ethynyl units and $\pi-\pi$ stacking distances of 3.22 and 3.27 Å between phenylethynylpyrrole units, which consist of two sp and 11 sp^2 atoms. Along the a axis, the phenylethynyl moieties stack in the same (syn-) direction with dihedral angles of 26.32° and 28.31° between ethynyl units and $\pi-\pi$ stacking distances of 3.71 and 3.82 Å between phenylethynylpyrrole units. Thus, anti-directional stacking is more effective than syn-directional stacking because of less steric hindrance. In polymorph **B** (Figure 4b), anti- and syn-directional stacking structures were observed with dihedral angles of 0° and 50.0° between ethynyl units, respectively, and the corresponding $\pi-\pi$ stacking distances of 3.49 and 3.90 Å, respectively. However, the overlapped area of the syn-directional stacking structure was more similar in the case of polymorph **B** compared to polymorph **A**. On the other hand, in polymorph **C** (Figure 4c), 1_2·Cl⁻ forms a zigzag-type stacking with two kinds of anti-directional stacking. In both anti-directional stacking structures, the dihedral angle between ethynyl units is 0° with the corresponding $\pi-\pi$ stacking distances of 3.19 and 3.90 Å. Therefore, the crystallization processes of polymorphs **A** and **B** may be different from that of polymorph **C**.

The *P*- and *M*-form chiral geometries of 1_2·Cl⁻ are derived from two nonorthogonally arranged receptor planes (Figure

DOI: 10.1021/acs.joc.6b01688
J. Org. Chem. 2016, 81, 8530−8536

Table 2. Hydrogen-Bonding Geometries in the Polymorphs of 1_2·Cl^-−TBA^+

polymorph	D−H···A	d(D···A)/Å
A	N1−H···Cl1	3.323
	N2−H···Cl1	3.336
	N3−H···Cl1	3.288
	N4−H···Cl1	3.307
	C14−H···Cl1	3.534
	C49−H···Cl1	3.516
	N5−H···Cl2	3.314
	N6−H···Cl2	3.274
	N7−H···Cl2	3.369
	N8−H···Cl2	3.283
	C84−H···Cl2	3.500
	C119−H···Cl2	3.514
B	N1−H···Cl	3.362
	N2−H···Cl	3.272
	N3−H···Cl	3.317
	N4−H···Cl	3.330
	C14−H···Cl	3.508
	C49−H···Cl	3.547
C	N1−H···Cl	3.394
	N2−H···Cl	3.273
	N3−H···Cl	3.356
	N4−H···Cl	3.279
	C14−H···Cl	3.460
	C49−H···Cl	3.452

5a). Although the resulting enantiomers were observed in a racemic state in the crystals, the arrangements of enantiomers differed between the polymorphs. In polymorph **A** (Figure 5b(i)), the *P*- and *M*-forms are alternately aligned along the *a* axis, whereas the identical chiral species are aligned along the *c* axis. In polymorph **B** (Figure 5b(ii)), the locations of *P*- and *M*-forms are similar to those in polymorph **A**, although the interactions between identical chiral species are weaker than those in polymorph **A**. In contrast, in polymorph **C** (Figure 5b(iii)), the enantiomers of $\mathbf{1}_2$·Cl^- are alternately arranged in a zigzag alignment.

Interfragment Interaction Energy. We performed *ab initio* electronic structure calculations for polymorphs **A**, **B**, and **C** using the fragment molecular orbital (FMO) method (FMO2-MP2/6-31G(d,p) level of the theory) and the interfragment interaction energies (IFIEs) among the four monomers using the GAMESS program package (Figures 6 and 7).[10,11] Note here that the Møller−Plesset second-order perturbation theory (MP2) can be used to evaluate both electrostatic and van der Waals interactions with high accuracy. Thus, the present scheme can be used for quantitative analyses of the interaction energy in organic crystals.

Table 3 shows the IFIE values among the four fragments. $IFIE_{12}$ and $IFIE_{34}$ are positive due to the repulsive interaction between two negatively charged receptor−anion complexes or two positively charged TBA cations. Comparison of the magnitudes of $IFIE_{12}$ and $IFIE_{34}$ reveals that the latter is larger than the former. This is because of the contact surface area between the neighboring monomers, wherein two TBA cations are quite distant from each other with less contact surface area and two receptor−anion complexes are partially in contact with hydrophobic moieties, resulting in the weak van der Waals

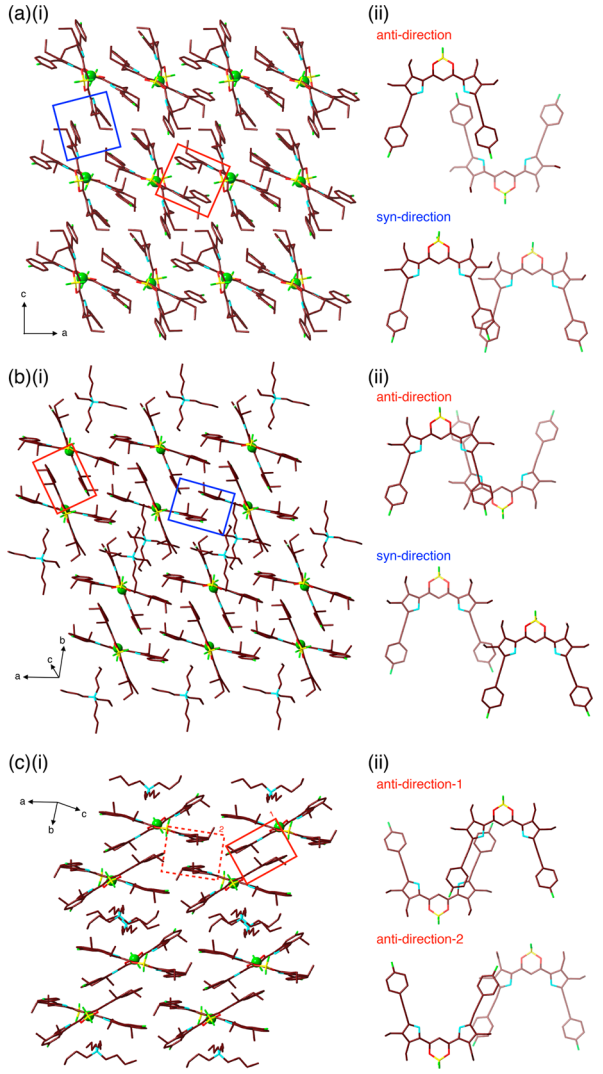

Figure 4. Views of (i) crystal packing and (ii) π−π stacking dimers for polymorphs (a) **A**, (b) **B**, and (c) **C**, wherein hydrogen atoms are omitted for clarity. Atom color code: brown, yellow, green, blue, and red refer to carbon, boron, fluorine, nitrogen, and oxygen, respectively.

interactions. However, other IFIEs are negative. In particular, the magnitudes of $IFIE_{13}$ and $IFIE_{24}$ of polymorph **C** are the largest among all of the IFIE values. This is because the receptor−anion complexes and the TBA cations of polymorph **C** are oriented face-to-face in a large contact surface area, resulting in the strong van der Waals interactions. In contrast to the scenario in polymorph **C**, the TBA cations in polymorphs **A** and **B** are oriented vertically toward the receptor−anion complexes and therefore do not have such strong interactions with the receptor−anion complexes. Therefore, we estimated that the polymorph **C** is more stable than polymorphs **A** and **B**. Although polymorph **A** has similar $IFIE_{13}$ and $IFIE_{24}$ compared to that of polymorph **B**, polymorph **B** contains more attractive interactions than polymorph **A**. Thus, the charge-segregated structure of polymorph **A** is less stable than polymorphs **B** and **C**.

SUMMARY

Three crystal polymorphs of ion-pairing assemblies were obtained from interlocked [2 + 1]-type receptor−anion complexes and TBA cations. Each of the polymorphs contained

DOI: 10.1021/acs.joc.6b01688
J. Org. Chem. 2016, 81, 8530−8536

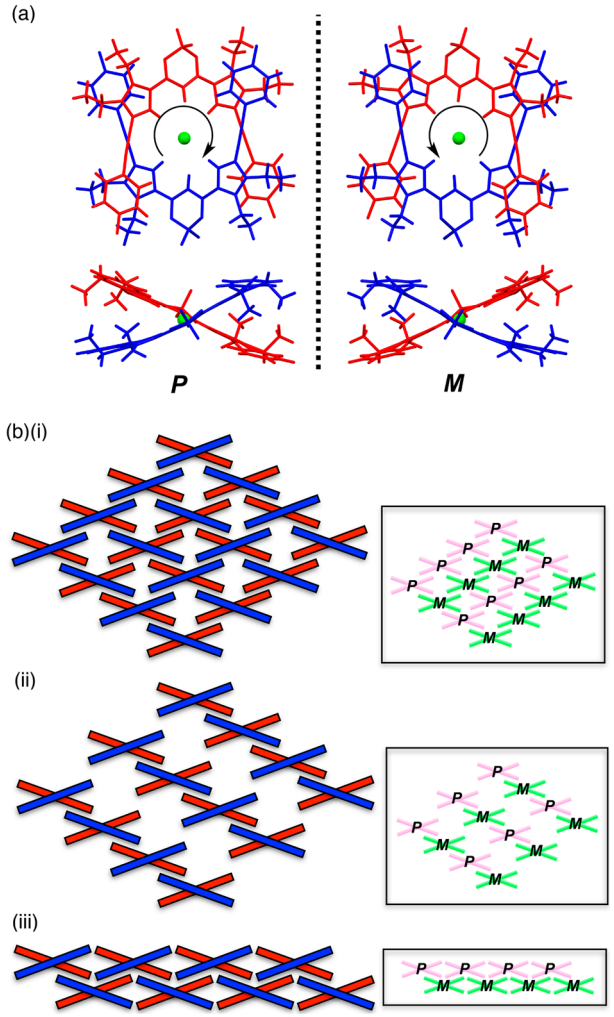

Figure 5. (a) Representation of chirality in $\mathbf{1}_2 \cdot Cl^-$ (top and side views); (b) arrangement of enantiomers in the polymorphs (i) **A**, (ii) **B**, and (iii) **C**.

totally charge-segregated and charge-by-charge assemblies. The solid-state ion-pairing assemblies had similar TBA cation geometries, whereas the geometries of the [2 + 1]-type receptor−anion complexes were correlated with the dihedral angles between the two receptors in the interlocked structures. Stacking interactions between π-electronic moieties also played important roles in controlling the assembly structures. Diverse arrangements of *P*- and *M*-configurations could be observed in the interlocked anion complexes of the polymorphs. Furthermore, a theoretical examination of the stabilities of the polymorphs was performed using the FMO method. Further investigations on the stabilities of polymorphs and their transformations are currently underway.

EXPERIMENTAL SECTION

Method for Single-Crystal X-ray Analysis. Crystallographic data for an ion pair $\mathbf{1}_2 \cdot Cl^- - TBA^+$, including the previously reported polymorph **A**,[4a] are summarized in Table 1. A single crystal of polymorph **A** was obtained by the vapor diffusion of *n*-hexane into an EtOAc solution of a 2:1 mixture of **1** and TBACl[4a] or by vapor diffusion of *n*-hexane into an EtOAc/(*S*)-(+)-2-butanol (5/1 (v/v)) solution of a 1:1 mixture of **1** and TBACl. A single crystal of polymorph **B** was obtained by vapor diffusion of *n*-hexane into an EtOAc/(*S*)-(−)-2-methyl-1-butanol (5/1 (v/v)) solution of the 1:1 mixture of **1** and TBACl. This data crystal was a red prism of the

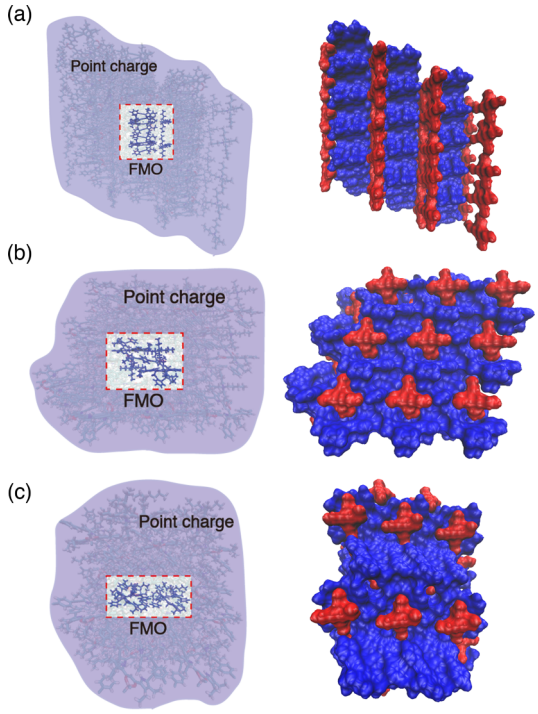

Figure 6. Model systems for the crystal polymorphs (a) **A**, (b) **B**, and (c) **C**. For the FMO calculations, the molecules inside the red dotted lines were treated quantum-mechanically and those in the purple surface as point charges (applicable areas visible in the top line of figures).

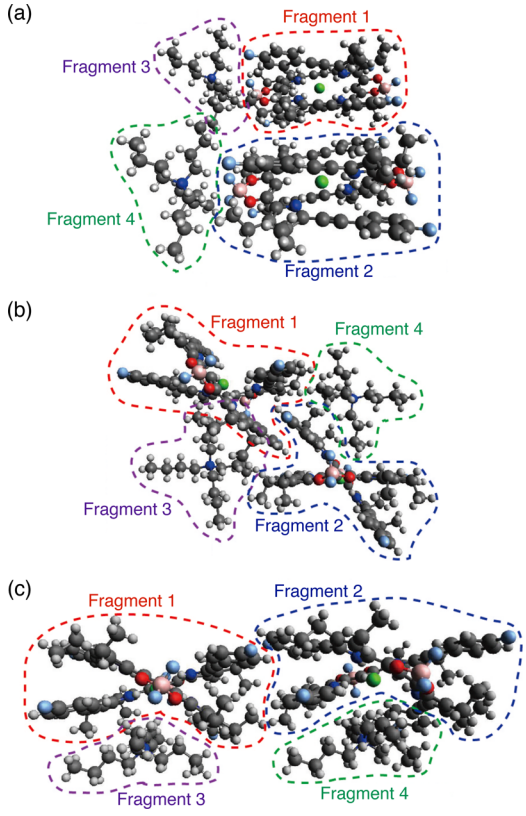

Figure 7. Definitions of fragments for (a) **A**, (b) **B**, and (c) **C** in FMO calculations.

DOI: 10.1021/acs.joc.6b01688
J. Org. Chem. 2016, 81, 8530−8536

Table 3. Interfragment Interaction Energy between *i*- and *j*-th Monomers ($IFIE_{ij}$) and Total IFIE

IFIE [kcal/mol]	A	B	C
$IFIE_{12}$	10.98	1.112	5.830
$IFIE_{13}$	−54.79	−53.04	−83.68
$IFIE_{14}$	−19.99	−34.91	−17.58
$IFIE_{23}$	−21.40	−26.61	−19.63
$IFIE_{24}$	−54.84	−53.28	−83.52
$IFIE_{34}$	27.05	22.80	20.80
Total	−113.0	−143.9	−177.8

approximate dimensions 0.12 mm × 0.06 mm × 0.06 mm. A single crystal of polymorph **C** was obtained by vapor diffusion of *n*-hexane into an EtOAc/(*rac*)-(±)-2-butanol (5/1 (v/v)) solution of a 1:1 mixture of **1** and TBACl. This data crystal was a red prism of the approximate dimensions 0.24 mm × 0.20 mm × 0.10 mm. For each crystal, data were collected at 93 K on a Rigaku XtaLAB P200 diffractometer with graphite monochromated Cu Kα radiation (λ = 1.54187 Å), and the structure was solved using the direct method. The non-hydrogen atoms were refined anisotropically. The calculations were performed using the Crystal Structure crystallographic software package of Molecular Structure Corporation.[12] CIF files (CCDC-1492732−1492733) can be obtained free of charge from the Cambridge Crystallographic Data Centre via www.ccdc.cam.ac.uk/data_request/cif.

DFT Calculations. Density functional theory (DFT) calculations of ion pairs were carried out using the Gaussian 09 program.[11] Three types of model structures were constructed from the single-crystal X-ray structures of polymorphs **A**, **B**, and **C** (Figure 6). These model structures were created using the modeling software, Mercury,[13] with the lattice repetition set at 3 × 3 × 3. Since there were several scrap molecules in the original structures, we eliminated them manually (see Supporting Figure 1 for all the model structures). The numbers of the $\mathbf{1}_2{\cdot}Cl^-$ (TBA cations) in the model structures of polymorphs **A**, **B**, and **C** were 75 (90), 54 (54), and 50 (60), respectively. Thus, their total charges were +15, 0, and +10, respectively. Each model system was divided into two parts: the central molecules that were treated quantum-mechanically and other environmental molecules surrounding the point charges estimated from individual monomer calculations at the MP2/6-31G(d,p) level (see Supporting Figures 3−6 and Supporting Tables 1−6 for their point charges of MM environment). In the quantum mechanical part, we detected a tetramer containing two $\mathbf{1}_2{\cdot}Cl^-$ (fragment 1 and 2) and two TBA cations (fragment 3 and 4) and assigned them as the four monomer fragments for FMO calculations (Figure 7).[14,15]

■ ASSOCIATED CONTENT

Supporting Information

The Supporting Information is available free of charge on the ACS Publications website at DOI: 10.1021/acs.joc.6b01688.

Spectroscopic data, X-ray crystallographic data, theoretical study (PDF)

Crystallographic data (CCDC 1492732−1492733) (CIF)

■ AUTHOR INFORMATION

Corresponding Authors

*E-mail: maedahir@ph.ritsumei.ac.jp.

*E-mail: shigeta@ccs.tsukuba.ac.jp.

Notes

The authors declare no competing financial interest.

■ ACKNOWLEDGMENTS

This work was supported by JSPS KAKENHI Grant Numbers JP26288042 for Scientific Research (B) and JP26107007 and JP26107004 for Scientific Research on Innovative Areas "Photosynergetics". Theoretical calculations were partially performed using the Research Center for Computational Science, Okazaki, Japan. We thank Prof. Atsuhiro Osuka, Dr. Hirotaka Mori, Mr. Koji Naoda, Mr. Shinichiro Ishida, and Mr. Takanori Soya, Kyoto University, for single-crystal X-ray analysis, and Prof. Hitoshi Tamiaki, Ritsumeikan University, for various measurements.

■ REFERENCES

(1) Selected examples of ion-based materials: (a) Wu, D. Q.; Liu, R. L.; Pisula, W.; Feng, X. L.; Müllen, K. *Angew. Chem., Int. Ed.* **2011**, *50*, 2791−2794. (b) Ren, Y.; Kan, W. H.; Henderson, M. A.; Bomben, P. G.; Berlinguette, C. P.; Thangadurai, V.; Baumgartner, T. *J. Am. Chem. Soc.* **2011**, *133*, 17014−17026. (c) Ren, Y.; Kan, W. H.; Thangadurai, V.; Baumgartner, T. *Angew. Chem., Int. Ed.* **2012**, *51*, 3964−3968. (d) Lee, J.-J.; Yamaguchi, A.; Alam, Md. A.; Yamamoto, Y.; Fukushima, T.; Kato, K.; Takata, M.; Fujita, N.; Aida, T. *Angew. Chem., Int. Ed.* **2012**, *51*, 8490−8494. (e) Soberats, B.; Yoshio, M.; Ichikawa, T.; Taguchi, S.; Ohno, H.; Kato, T. *J. Am. Chem. Soc.* **2013**, *135*, 15286−15289. (f) Krikorian, M.; Liu, S.; Swager, T. M. *J. Am. Chem. Soc.* **2014**, *136*, 2952−2955. (g) Soberats, B.; Uchida, E.; Yoshio, M.; Kagimoto, J.; Ohno, H.; Kato, T. *J. Am. Chem. Soc.* **2014**, *136*, 9552−9555.

(2) Ion-pairing assemblies of π-electronic anions: (a) Maeda, H.; Fukui, A.; Yamakado, R.; Yasuda, N. *Chem. Commun.* **2015**, *51*, 17572−17575. (b) Bando, Y.; Haketa, Y.; Sakurai, T.; Matsuda, W.; Seki, S.; Takaya, H.; Maeda, H. *Chem. - Eur. J.* **2016**, *22*, 7843−7850.

(3) Reviews on ion-based assemblies comprising the receptor−anion complexes: (a) Dong, B.; Maeda, H. *Chem. Commun.* **2013**, *49*, 4085−4099. (b) Maeda, H. *Bull. Chem. Soc. Jpn.* **2013**, *86*, 1359−1399.

(4) (a) Yamakado, R.; Sakurai, T.; Matsuda, W.; Seki, S.; Yasuda, N.; Akine, S.; Maeda, H. *Chem. - Eur. J.* **2016**, *22*, 626−638. (b) Yamakado, R.; Maeda, H. *J. Photochem. Photobiol. A* **2016**, in press (DOI: 10.1016/j.jphotochem.2015.10.013).

(5) The data have been updated from the previous examinations in ref 4a: Yamakado, R.; Ashida, Y.; Maeda, H. To be submitted.

(6) (a) Wisner, J. A.; Beer, P. D.; Drew, M. G. B. *Angew. Chem., Int. Ed.* **2001**, *40*, 3606−3609. (b) Ng, K.-Y.; Cowley, A. R.; Beer, P. D. *Chem. Commun.* **2006**, 3676−3678. (c) Schulze, B.; Friebe, C.; Hager, M. D.; Günther, W.; Köhn, U.; Jahn, B. O.; Görls, H.; Schubert, U. S. *Org. Lett.* **2010**, *12*, 2710−2713. (d) Hirsch, B. E.; McDonald, K. P.; Qiao, B.; Flood, A. H.; Tait, S. L. *ACS Nano* **2014**, *8*, 10858−10869. (e) Robinson, S. W.; Mustoe, C. L.; White, N. D.; Brown, A.; Thompson, A. L.; Kennepohl, P.; Beer, P. D. *J. Am. Chem. Soc.* **2015**, *137*, 499−507.

(7) Bernstein, J. *Polymorphism in Molecular Crystals*; Clarendon Press: Oxford, 2002.

(8) Selected examples: (a) Zhang, G.; Yang, G.; Wu, N.; Ma, J. S. *Cryst. Growth Des.* **2006**, *6*, 229−234. (b) Martins, D. M. S.; Middlemiss, D. S.; Pulham, C. R.; Wilson, C. C.; Weller, M. T.; Henry, P. F.; Shankland, N.; Shankland, K.; Marshall, W. G.; Ibberson, R. M.; Knight, K.; Moggach, S.; Brunelli, M.; Morrison, C. A. *J. Am. Chem. Soc.* **2009**, *131*, 3884−3893. (c) Kukovec, B.-M.; Vaz, P. D.; Calhorda, M. J.; Popovíc, Z. *Cryst. Growth Des.* **2010**, *10*, 3685−3693. (d) Thomas, L. H.; Craig, G. A.; Gutmann, M. J.; Parkin, A.; Shankland, K.; Wilson, C. C. *CrystEngComm* **2011**, *13*, 3349−3354. (e) Pick, A.; Klues, M.; Rinn, A.; Klaus, H.; Chatterjee, S.; Witte, G. *Cryst. Growth Des.* **2015**, *15*, 5495−5504.

(9) (a) Miura, H.; Ushio, T.; Nagai, K.; Fujimoto, D.; Lepp, Z.; Takahashi, H.; Tamura, R. *Cryst. Growth Des.* **2003**, *3*, 959−965. (b) Martins, F. T.; deLima, P. V.; Azarias, L. C.; de Abreu, P. J.; Neves, P. P.; Legendre, A. O.; de Andrade, F. M.; de Oliveira, G. R.; Ellena, J.; Doriguetto, A. C. *CrystEngComm* **2011**, *13*, 5737−5743.

DOI: 10.1021/acs.joc.6b01688
J. Org. Chem. 2016, 81, 8530−8536

(10) Schmidt, M. W.; Baldridge, K. K.; Boatz, J. A.; Elbert, S. T.; Gordon, M. S.; Jensen, J. H.; Koseki, S.; Matsunaga, N.; Nguyen, K. A.; Su, S. J.; Windus, T. L.; Dupuis, M.; Montgomery, J. A. *J. Comput. Chem.* **1993**, *14*, 1347−1363.
(11) Frisch, M. J.; Trucks, G. W.; Schlegel, H. B.; Scuseria, G. E.; Robb, M. A.; Cheeseman, J. R.; Scalmani, G.; Barone, V.; Mennucci, B.; Petersson, G. A.; Nakatsuji, H.; Caricato, M.; Li, X.; Hratchian, H. P.; Izmaylov, A. F.; Bloino, J.; Zheng, G.; Sonnenberg, J. L.; Hada, M.; Ehara, M.; Toyota, K.; Fukuda, R.; Hasegawa, J.; Ishida, M.; Nakajima, T.; Honda, Y.; Kitao, O.; Nakai, H.; Vreven, T.; Montgomery, J. A., Jr.; Peralta, J. E.; Ogliaro, F.; Bearpark, M.; Heyd, J. J.; Brothers, E.; Kudin, K. N.; Staroverov, V. N.; Kobayashi, R.; Normand, J.; Raghavachari, K.; Rendell, A.; Burant, J. C.; Iyengar, S. S.; Tomasi, J.; Cossi, M.; Rega, N.; Millam, J. M.; Klene, M.; Knox, J. E.; Cross, J. B.; Bakken, V.; Adamo, C.; Jaramillo, J.; Gomperts, R.; Stratmann, R. E.; Yazyev, O.; Austin, A. J.; Cammi, R.; Pomelli, C.; Ochterski, J. W.; Martin, R. L.; Morokuma, K.; Zakrzewski, V. G.; Voth, G. A.; Salvador, P.; Dannenberg, J. J.; Dapprich, S.; Daniels, A. D.; Farkas, Ö.; Foresman, J. B.; Ortiz, J. V.; Cioslowski, J.; Fox, D. J. *Gaussian 09*, revision D.01; Gaussian, Inc., Wallingford, CT, 2013.
(12) *CrystalStructure*, Ver. 3.8; Single Crystal Structure Analysis Software, Rigaku/MSC and Rigaku Corporation: 2006.
(13) Macrae, C. F.; Edgington, P. R.; McCabe, P.; Pidcock, E.; Shields, G. P.; Taylor, R.; Towler, M.; Van De Streek, J. *J. Appl. Crystallogr.* **2006**, *39*, 453−457.
(14) Kitaura, K.; Ikeo, E.; Asada, T.; Nakano, T.; Uebayasi, M. *Chem. Phys. Lett.* **1999**, *313*, 701−706.
(15) Nakano, T.; Kaminuma, T.; Sato, T.; Fukuzawa, K.; Akiyama, Y.; Uebayasi, M.; Kitaura, K. *Chem. Phys. Lett.* **2002**, *351*, 475−480.

DOI: 10.1021/acs.joc.6b01688
J. Org. Chem. 2016, 81, 8530−8536